

EFFECT OF FINE BUBBLES ON FLOW PROPERTIES IN BUBBLE COLUMN WITH SUSPENDED SOLID PARTICLES

SHIGEHARU MOROOKA, TETSUYA MIZOGUCHI, TOKIHIRO KAGO
AND YASUO KATO

Department of Applied Chemistry, Kyushu University, Fukuoka 812

NOBUYUKI HIDAKA

Department of Chemical Engineering, Kagoshima University, Kagoshima 890

Key Words: Chemical Reactor, Energy, Coal, Coal Liquefaction, Dissolver, Bubble Column, Dispersion, Mixing, Particle, Gas Holdup

Flow properties in a dissolver for direct coal liquefaction were simulated by using a cold bubble column of 12 cm i.d. To generate small gas bubbles in the column, a surfactant was added to tap water and a gas distributor with fine holes was employed. When glass spheres of 44 and 113 μm dia. were suspended in the presence of the surfactant, the gas holdup was 1.5–4 times that for the tap water system, and the axial dispersion coefficient of liquid showed a minimum at superficial gas velocities of 3–5 $\text{cm} \cdot \text{s}^{-1}$. The mean settling velocity of solid particles, v_p , was affected by the quality of flow in addition to gas velocity and terminal velocity of solid particles. Most values of v_p obtained in this experiment were larger than those for the tap water system where no fine gas bubbles were generated. Experimental equations for the correlation of v_p are presented.

An introduction of secondary gas in the homogeneous bubble flow regime effectively increased the axial liquid mixing. This suggests that in the design of a dissolver quenching gas injection is important to attain spontaneous discharge of ash particles from the top of the vessel.

Introduction

In a dissolver for direct coal liquefaction, mineral matter such as CaCO_3 , FeS_2 and SiO_2 are likely to form agglomerates and accumulate at the reactor bottom.¹⁷⁾ If the axial liquid mixing is sufficiently large, however, these solid particles can be spontaneously discharged from the outlet at the top of the column even at low liquid velocities.¹⁰⁾ Thus the understanding of flow properties is an important factor in the design and operation of the dissolver.

The axial concentration distribution of solid particles in bubble columns has been investigated by many authors.^{3,5,7,15)} Kato *et al.*^{5,7)} described the axial concentration distribution with a sedimentation-dispersion model, and correlated the axial dispersion coefficients of liquid and solid particles and the mean settling velocity of solid particles.

Under the conditions of direct coal liquefaction, the gas holdup in the dissolver is much larger than that for air–water systems in the heterogeneous bubble flow and turbulent flow regime.^{2,8,9,12,13,16)} The axial liquid mixing measured in dissolvers of SRC^{11,12)} and EDS¹⁶⁾ processes is also quite different from that in

the air–water systems.^{6,7)} Therefore, the flow pattern in the dissolver at lower gas velocities seems to belong to the homogeneous bubble flow regime, where small gas bubbles with a narrow size distribution ascend at nearly the same rising velocities. However, the data of liquid mixing in dissolvers are not confirmed, and the characterization of homogeneous bubble flow is quite insufficient.

In this study, interfacial properties of water are changed by adding a surfactant and the characteristic flow in dissolvers is simulated in a cold flow model reactor. Gas holdup and axial liquid mixing in the homogeneous bubble flow regime are determined as functions of gas and liquid velocities. The effects of the presence of suspended solid particles and the interfacial property of liquid are also studied.

1. Experimental

Figure 1 shows the bubble column with suspended solid particles. The main column was 12 cm in i.d. and 205 or 226.5 cm high, and was made of an acrylic plastic pipe. Air was used as the gas phase and was introduced through two distributors. The primary gas distributor was a perforated plate 3 mm thick, having 85 holes of 1 mm dia. A bronze net of 65 mesh was put on the perforated plate to prevent the fall of solid particles. The mesh was partially clogged by solid

Received May 1, 1986. Correspondence concerning this article should be addressed to S. Morooka. T. Mizoguchi is now with Toyo Soda Mfg. Co., Ltd. Y. Kato is Professor Emeritus, Kyushu University.

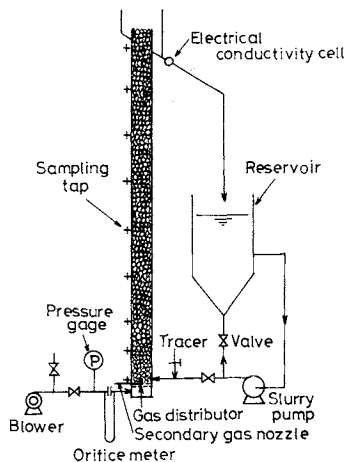


Fig. 1. Schematic diagram of experimental apparatus.

particles. The secondary gas distributor was a 3 or 6 mm i.d. single nozzle which was fixed 4 cm above the plate at the center of the cross section.

The liquid phase was tap water containing a surfactant (100 ppm of Triton X405; polyoxyethylene-*p*-iso-octylphenyl ether, Rohm & Haas). Tap water without the additive was also used. The solid phase was sieved glass spheres (density = 2500 kg · m⁻³) with an average diameter of 44, 113 and 230 μm.

After steady state was attained, the slurry was sampled from sampling taps on the wall. The solid concentration was obtained by weighing dried particles in each sample.

The axial dispersion coefficient of liquid was measured by the impulse response method. About 5 ml of a 2 kmol · m⁻³ KCl solution was injected at the inlet and was detected by an electric conductivity cell at the outlet. The gas holdup was calculated from the gas volume in the column after the gas and liquid flows were interrupted simultaneously.

Table 1 shows the experimental conditions. The surface tension of water in the presence of the surfactant was 0.055 N · m⁻¹. Experiments were carried out at temperatures between 287–303 K.

2. Experimental Results and Discussion

2.1 Gas holdup

Figure 2 shows the relationship between gas holdup and superficial gas velocity. The data obtained in dissolvers of EDS,¹⁶⁾ SRC¹²⁾ and IG⁸⁾ processes are also shown in the figure. When the surfactant is added and solid particles of 44 or 113 μm dia. are suspended in the range of $U_g < 6 \text{ cm} \cdot \text{s}^{-1}$, small bubbles of about 2 mm dia. are produced without coalescence. As a result homogeneous bubble flow prevails in the bed. The gas holdup is 1.5–4 times larger than that for the tap water system without the addition of surfactant and is about the same as in actual dissolvers. The gas holdup increases with increasing gas velocity and

Table 1. Experimental conditions

d_p [μm]	\bar{C} [Mg · m ⁻³]	U_l [cm · s ⁻¹]	Key	
			W	T
44	0.05–0.1	0.2	○	●
44		0.5	⊙	⊗
44		1.0	⊖	⊕
44	0.17	0.5	⊕	⊗
113	0.05–0.1	0.4	□	■
113		1.0	⊠	⊡
230	0.05–0.1	0.6	△	▲
230		2.0	▽	▼
230		3.0	△	▲
230		4.0	△	▲

W, tap water; T, 100 ppm Triton X-405 solution.

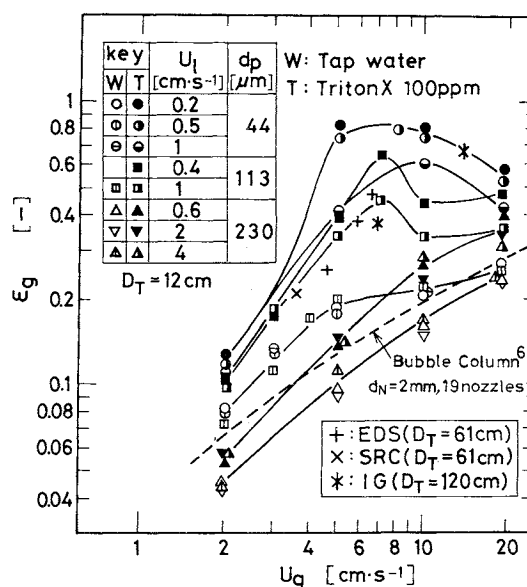


Fig. 2. Effect of gas velocity on gas holdup.

decreases with increasing liquid velocity.

In the range of $U_g > 6 \text{ cm} \cdot \text{s}^{-1}$, gas bubbles in the surfactant-containing water begin to coalesce. The gas holdup decreases with increasing gas velocity, and the flow regime changes to heterogeneous bubble flow and then to turbulent flow.

When solid particles of 230 μm dia. are suspended, coalescence of bubbles occurs in spite of the addition of the surfactant. The gas holdup is 1.2–1.5 times larger than that for the tap water system without the addition of surfactant. The effect of superficial liquid velocity on gas holdup for $d_p = 230 \text{ μm}$ is negligible in the range of $U_l < 4 \text{ cm} \cdot \text{s}^{-1}$.

2.2 Liquid mixing

Figure 3 shows the longitudinal dispersion coefficient of liquid in the bubble column with suspended solid particles, E_{sl} . With increasing gas velocity, E_{sl} in the presence of the surfactant first decreases, passes

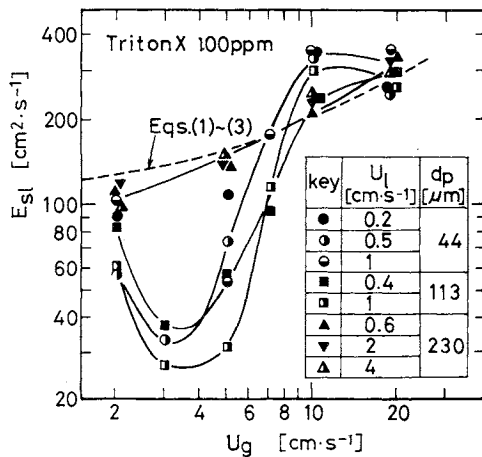


Fig. 3. Effect of gas velocity on E_{sl} .

the minimum value and then increases.

Kato and Nishiwaki⁶⁾ correlated the axial dispersion coefficient of liquid for the air-water system in the heterogeneous bubble flow and turbulent bubble flow regime by the following equations.

$$\frac{(U_g D_T / E_l)}{(\epsilon_g^* / \epsilon_g)^\alpha} = \frac{13(U_g / \sqrt{g D_T})}{1 + 6.5(U_g / \sqrt{g D_T})^{0.8}} \quad (1)$$

$$\epsilon_g^* = \frac{U_g}{31 + 4.5 U_g^{0.8} \{1 - \exp(-0.040 U_g^{1.8})\}} \quad (2)$$

$$\alpha = 1 - \exp(-0.2 U_g^2) \quad (3)$$

where the superficial gas velocity, U_g , is expressed in the unit of $\text{cm} \cdot \text{s}^{-1}$. The broken line in Fig. 3 shows the values calculated from Eqs. (1)–(3). In the range of $U_g = 3\text{--}5 \text{ cm} \cdot \text{s}^{-1}$, the experimental values of E_{sl} in the presence of the surfactant are 1/2–1/5 those of Kato and Nishiwaki.⁶⁾ When the solid particles of $230 \mu\text{m}$ are suspended in the presence of the surfactant, however, the value of E_{sl} is nearly in agreement with Eqs. (1)–(3). This means that the presence of coarser solid particles causes the coalescence of gas bubbles.

Figure 4 shows the correlation of E_{sl} . The definitions of the coordinates are identical with that of Kato *et al.*⁶⁾ The experimental values of E_{sl} in the homogeneous bubble flow regime can be expressed by the solid line, while those for the tap water system are well expressed by Eqs. (1)–(3).

Figure 5 shows the correlation of E_{sl} obtained in dissolvers for direct coal liquefaction. These data are in agreement with the solid line, which expresses the correlation of E_{sl} in the presence of the surfactant. The values of E_l obtained by Aoyama *et al.*¹⁾ and Kato⁴⁾ show the same tendency as the solid line. However, the axial dispersion coefficient of liquid in the presence of the surfactant is strongly dependent on liquid properties and gas distributor type. Schügerl

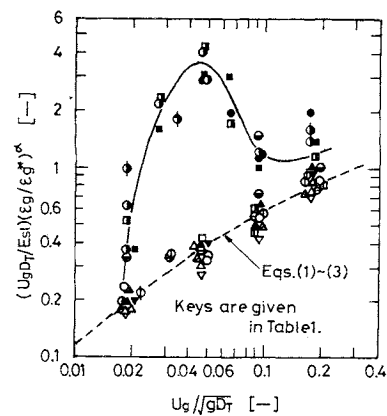


Fig. 4. Correlation of E_{sl} .

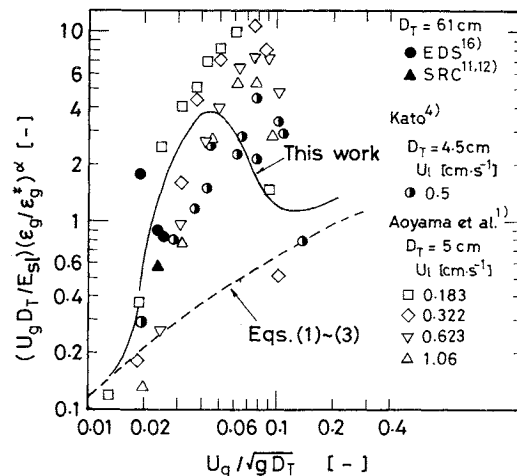


Fig. 5. Correlation of E_{sl} and E_l in literature.

*et al.*¹⁴⁾ also reported the complex effects of additives and gas distributors.

2.3 Secondary gas

The secondary gas which is introduced through a single nozzle produces large bubbles. These bubbles ascend along the central axis of the column, inducing an upward flow in the central region and a downward flow in the peripheral region.

Figure 6 shows the effect of the secondary gas velocity on the gas holdup and the axial dispersion coefficient of liquid. The total superficial gas velocity, $(U_g + U_{gs})$, is fixed at 3 and $4 \text{ cm} \cdot \text{s}^{-1}$. The gas holdup decreases with increasing secondary gas velocity. The value of E_{sl} increases with increasing secondary gas velocity and becomes equivalent to that of the heterogeneous bubble flow when U_{gs} exceeds about $0.5 \text{ cm} \cdot \text{s}^{-1}$. This means that the axial liquid mixing is much affected by internal recirculation flow, which is easily induced by a small amount of coalesced bubbles. In this sense, the solid line in Fig. 4 indicates a typical correlation of E_{sl} in the homogeneous bubble flow regime. The value of E_{sl} under other circumstances varies between the solid and broken lines in Fig. 4.

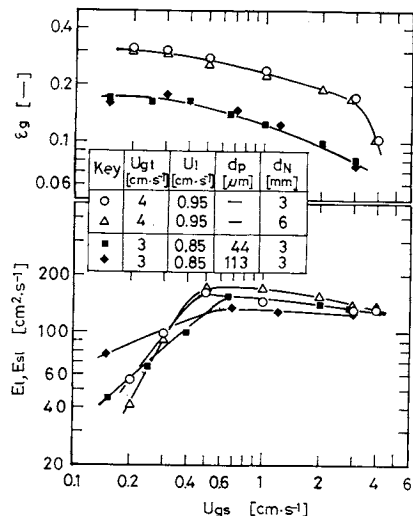


Fig. 6. Effect of secondary gas flow on gas holdup and liquid mixing.

2.4 Axial concentration distribution of solid particles

If the concentration of solid particles is low, the settling velocity of solid particles, v_p , is not affected by the local solid concentration, C , which is then expressed as follows:^{5,7)}

$$C = \left(C_0 + \frac{u_l}{v_p - u_l} C^* \right) \exp \left\{ \frac{-(v_p - u_l)}{E_p} z \right\} - \frac{u_l}{v_p - u_l} C^*$$

$$= \left(C_L + \frac{u_l}{v_p - u_l} C^* \right) \exp \left\{ \frac{v_p - u_l}{E_p} (L - z) \right\} - \frac{u_l}{v_p - u_l} C^*$$
(4)

where C_0 and C_L are the solid concentration extrapolated to $z=0$ and $z=L$, respectively. C^* is the solid concentration in the feed.

Figure 7 shows examples of the axial concentration distribution of solid particles. The axial concentration gradient in the presence of the surfactant is generally larger than that for the tap water system and becomes maximum at $U_g = 3\text{--}5\text{ cm}\cdot\text{s}^{-1}$. Figure 8 also illustrates how the secondary gas flow improves the axial concentration distribution of solid particles in the column.

2.5 Mean settling velocity of solid particles

When solid particles of $230\text{ }\mu\text{m}$ were suspended, ϵ_g and E_{sl} were not affected by the liquid velocity, as shown in Figs. 2 and 3. Then E_p and v_p were calculated separately from Eq. (4) by using the linear relationship between $(v_p - u_l)/E_p$ and u_l . The value of E_p obtained in this way was in agreement with E_{sl} as determined by the impulse response method. Solid particles smaller than $230\text{ }\mu\text{m}$ are supposed to behave more like liquid phase.⁵⁾ Therefore, the axial dispersion coefficient of solid particles can be approximated by that of liquid in the range of the present experiment. With this assumption, v_p is the only unknown parameter in Eq. (4) and is obtained by comparing an experimental concentration distribution of solid par-

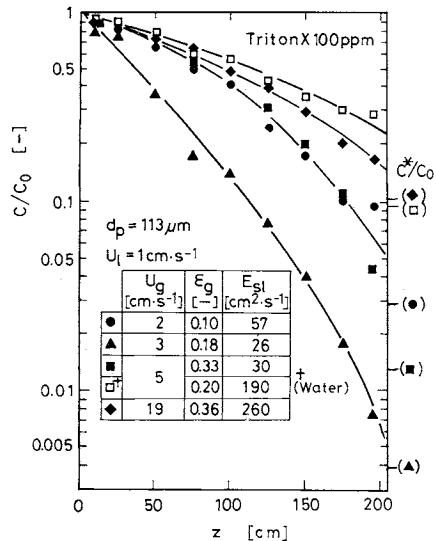


Fig. 7. Axial concentration distributions of solid particles.

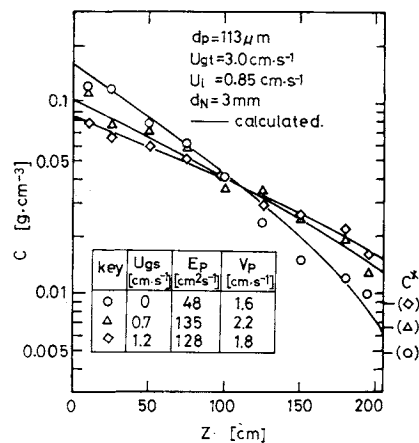


Fig. 8. Effect of secondary gas flow on axial concentration distribution of solid particles.

ticles with Eq. (4).

Figure 9 shows the mean settling velocity normalized with the terminal velocity of a solid particle on the basis of the correlation of Kato *et al.*^{5,7)} The solid lines indicate v_p in the presence of the surfactant, while the chain line shows that for the tap water system. The broken line is the correlation of Kato *et al.*⁵⁾ in the heterogeneous flow and turbulent flow regime and is calculated from

$$v_p = v_t \{ 1 + 1.5(U_g/v_t) \}^{0.30} \psi_i^{2.5} \quad (5)$$

Most of the values obtained in this experiment are larger than those from Eq. (5). Especially, the mean settling velocity in the presence of the surfactant deviates nonlinearly from Eq. (5) and is strongly affected by the quality of flow as well as the terminal velocity of solid particles and superficial gas velocity. The quality of flow is dependent on type of gas distributor, properties of the liquid, column size and gas and liquid velocities.

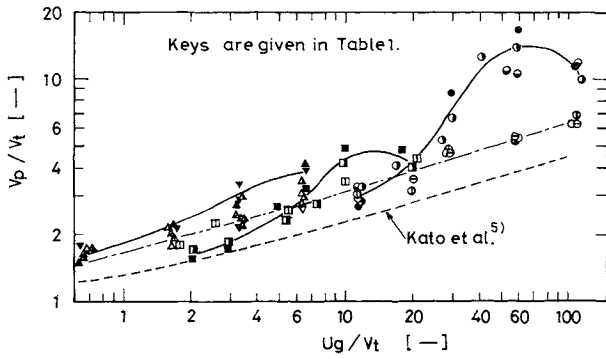


Fig. 9. Relationship between v_p/v_t and U_g/v_t .

Figure 10 shows the effects of particle diameter and gas holdup on $(v_p - v_t)/v_t$. The value of $(v_p - v_t)/v_t$ increases with increasing gas holdup and with decreasing mean particle diameter.

Figure 11 shows the correlation of v_p in the homogeneous bubble flow regime, and the following experimental equation is obtained.

$$v_p/v_t = 1 + 3.5 \varepsilon_g (d_p v_t / v_l)^{-0.55} \quad (6)$$

where the gas holdup is a function of superficial gas velocity and other factors and can be estimated from Fig. 2.

Figure 12 is the correlation of v_p in the heterogeneous bubble flow and turbulent flow regime. The solid line in Fig. 12 is expressed by the following equation.

$$v_p/v_t = 1 + 10 \varepsilon_g (d_p v_t / v_l)^{-0.25} \quad (7)$$

Values obtained by Kato *et al.*⁷⁾ and Smith and Ruether¹⁵⁾ are roughly in agreement with Eq. (7).

Conclusion

Flow characteristics in dissolvers for direct coal liquefaction processes were simulated in a cold flow model reactor by producing small gas bubbles in the presence of a nonionic surfactant.

The gas holdup decreased with increasing particle diameter. With solid particles of 44 or 113 μm dia., the gas holdup decreased with increasing liquid velocity.

The longitudinal dispersion coefficient of liquid in the presence of a surfactant was 1/5–3/2 that for the tap water system, and showed a minimum in the range of $U_g = 3\text{--}5 \text{ cm} \cdot \text{s}^{-1}$. When solid particles of 230 μm dia. were suspended, however, the liquid mixing was approximately in agreement with that for the tap water system.

The introduction of secondary gas in the homogeneous bubble flow regime effectively increased the axial mixing of liquid and solid. This indicates that the design of quenching gas injection in a dissolver plays an important role in avoiding the accumulation of ash particles at the dissolver bottom.

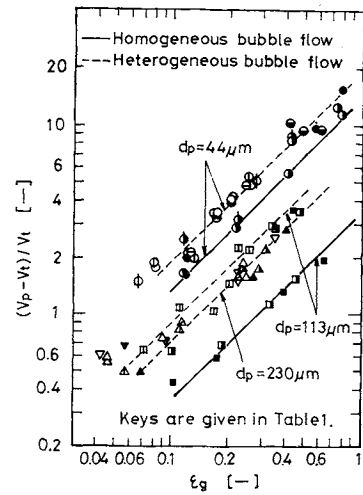


Fig. 10. Effects of particle diameter and gas holdup on v_p .

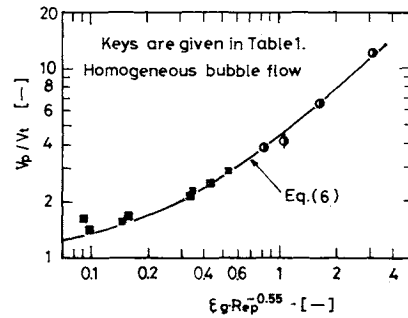


Fig. 11. Correlation of v_p in homogeneous bubble flow regime.

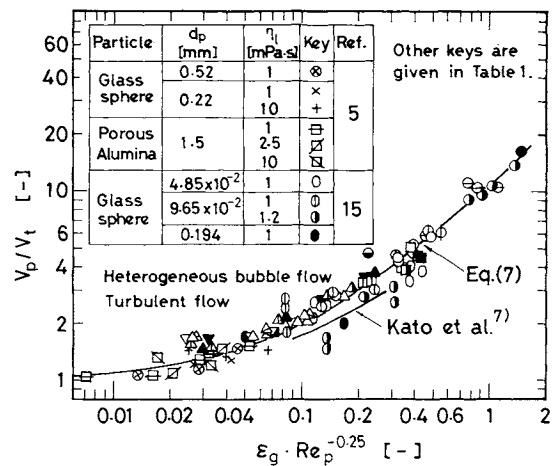


Fig. 12. Correlation of v_p in heterogeneous bubble flow and turbulent flow regime.

The mean settling velocity of solid particles in the homogeneous bubble flow regime was correlated by Eq. (6). The value of v_p in the heterogeneous bubble flow and turbulent flow regime was expressed by Eq. (7). However, more research is needed to clarify the boundary between the homogeneous bubble flow regime and the heterogeneous bubble flow and turbulent flow regime.

Acknowledgment

This work was supported by a Grant-in-Aid for Energy Research (No. 60040005) from the Ministry of Education, Science and Culture of Japan.

Nomenclature

C	= local concentration of solid particles in slurry	
		$[\text{kg} \cdot \text{m}^{-3}]$
C_0	= C extrapolated to $z=0$	$[\text{kg} \cdot \text{m}^{-3}]$
C_L	= C extrapolated to $z=L$	$[\text{kg} \cdot \text{m}^{-3}]$
C^*	= C in feed	$[\text{kg} \cdot \text{m}^{-3}]$
\bar{C}	= C averaged in column	$[\text{kg} \cdot \text{m}^{-3}]$
D_T	= column diameter	$[\text{m}]$
d_N	= nozzle diameter	$[\text{m}]$
d_p	= mean particle diameter	$[\text{m}]$
E_l	= longitudinal dispersion coefficient of liquid	$[\text{m}^2 \cdot \text{s}^{-1}]$
E_p	= longitudinal dispersion coefficient of solid particles	$[\text{m}^2 \cdot \text{s}^{-1}]$
E_{st}	= longitudinal dispersion coefficient of liquid in slurry	$[\text{m}^2 \cdot \text{s}^{-1}]$
L	= column height	$[\text{m}]$
Re_p	= Reynolds number, $d_p v_i / \nu_l$	$[-]$
U_g	= superficial velocity of primary gas	$[\text{m} \cdot \text{s}^{-1}]$
U_{gs}	= superficial velocity of secondary gas	$[\text{m} \cdot \text{s}^{-1}]$
U_{gt}	= $U_g + U_{gs}$	$[\text{m} \cdot \text{s}^{-1}]$
U_l	= superficial velocity of slurry	$[\text{m} \cdot \text{s}^{-1}]$
u_i	= actual velocity of slurry, $U_l / (1 - \epsilon_g)$	$[\text{m} \cdot \text{s}^{-1}]$
v_p	= mean settling velocity of solid particles	$[\text{m} \cdot \text{s}^{-1}]$
v_t	= terminal velocity of solid particle	$[\text{m} \cdot \text{s}^{-1}]$
z	= axial coordinate	$[\text{m}]$
α	= exponent defined by Eq. (3)	$[-]$
ϵ_g	= gas holdup	$[-]$
ϵ_g^*	= gas holdup defined by Eq. (2)	$[-]$
η_l	= liquid viscosity	$[\text{Pa} \cdot \text{s}]$

ν_l	= kinematic liquid viscosity	$[\text{m}^2 \cdot \text{s}^{-1}]$
ψ_i	= liquid fraction in slurry	$[-]$

Literature Cited

- 1) Aoyama, Y., K. Ogushi, K. Koide and H. Kubota: *J. Chem. Eng. Japan*, **1**, 158 (1968).
- 2) Idogawa, K., M. Ikeda, T. Fukuda and S. Morooka: *Kagaku Kogaku Ronbunshu*, **12**, 107 (1986).
- 3) Kara, S., B. G. Kelkar, Y. T. Shah and N. L. Carr: *Ind. Eng. Chem. Process Des. Dev.*, **21**, 584 (1982).
- 4) Kato, Y.: *Kagaku Kōgaku*, **27**, 887 (1963).
- 5) Kato, Y., S. Morooka, T. Kago, T. Saruwatari and S.-Z. Yang: *J. Chem. Eng. Japan*, **18**, 308 (1985).
- 6) Kato, Y. and A. Nishiwaki: *Kagaku Kōgaku*, **35**, 912 (1971); *Int. Chem. Eng.*, **12**, 182 (1972).
- 7) Kato, Y., A. Nishiwaki, T. Fukuda and S. Tanaka: *J. Chem. Eng. Japan*, **5**, 112 (1972).
- 8) Kürten, H.: *Chem.-Ing.-Tech.*, **54**, 409 (1982).
- 9) Mochida, N.: '85 Int. Chem. Plant Eng. Exhib. Conf., Tokyo (1985).
- 10) Morooka, S., Y. Kato, S. Ikejiri, M. Nakajima and H. Matsuyama: *J. Chem. Eng. Japan*, **19**, 137 (1986).
- 11) Panvelkar, S. V., J. W. Tierney and Y. T. Shah: *Chem. Eng. Sci.*, **37**, 1582 (1982).
- 12) Pittsburg & Midway Coal Mining Co.: DOE PC/50046-9 (1984).
- 13) Sangnimmuan, A., G. N. Prasad and J. B. Agnew: *Chem. Eng. Commun.*, **25**, 193 (1984).
- 14) Schügerl, K., J. Lücke and U. Oels: *Adv. Biochem. Eng.*, **7**, 1 (1977).
- 15) Smith, D. N. and J. A. Ruether: *Chem. Eng. Sci.*, **40**, 741 (1985).
- 16) Tarmy, B., M. Chang, C. Coualoglou and P. Ponzi: *Chem. Engr.*, Oct., 18 (1984).
- 17) Ying, D. H. S., R. Sivasubramanian, S. F. Moujaes and E. N. Givens: DOE ET/14801-30 (1982).